BUOYANCY-DRIVEN NATURAL VENTILATION OF A ROOM WITH LARGE OPENINGS

Rong Li[1], Adrian Pitts[1], and Yuguo Li[2]

[1]School of Architecture, the University of Sheffield,
Sheffield, S10 2TN, UK
[2]Department of Mechanical Engineering, the University of Hong Kong, China

ABSTRACT

The buoyancy-driven natural ventilation of a room with large lower and higher level openings is investigated by both theoretical analysis and CFD simulation. Pressure-based formulae are developed for the prediction of the height of neutral plane and airflow rate, and three different flow modes are identified according to the position of the neutral level: (I) when the neutral height is at intermediate level of the lower opening; (II) when the neutral height has no intersection with openings; (III) when the neutral height is at the intermediate level of the higher opening. CFD simulation is then performed to cross-check the validity of the formulae derived. Good agreement is achieved for the airflows of flow mode (I) both quantitatively and qualitatively, and the discrepancy is less than 18% for neutral level prediction and 7% for airflow rate prediction. But poor agreement is observed for flow mode (III) with discrepancies over 30% at some points, although the predictions on airflow rate generally show the same trend. Guidelines are also developed in relation to the opening design based on the analytical model developed and the CFD simulation.

KEYWORDS

Natural ventilation; Buoyancy forces; CFD; Large openings; Neutral plane;

INTRODUCTION

The performance of natural ventilation driven by buoyancy forces in a single-zone room is considered in this paper. This is a very simple physical model of many realistic buildings with buoyancy-driven airflow (Figure 1), such as atrium spaces, industrial and agriculture buildings. The appliances or occupants or other equipments located at the bottom of the room act as the heat source and usually two openings are employed in the model, typically one at higher level with the other at lower level. All other walls are assumed to be adiabatic.

The airflow for this model is commonly characterized as the displacement ventilation. The heat source warms the internal air which buoys up resulting in a higher pressure at the upper zone and a lower pressure at the lower zone. As a consequence, the inside air goes out through the upper opening and outside air comes in through the lower opening. Numerous models have been developed for this type of ventilation focusing on various situations with different distributions of heat sources or air temperatures, including those by Li (2000), Anderson (2003) and Linden et al. (1990). Chen and Li (2002) and Fitzgerald and Woods (2004) also investigated the situation where an additional intermediate opening is introduced. These studies all assume that the openings have a negligible height, i.e. the pressure is uniformly distributed for the whole opening height.

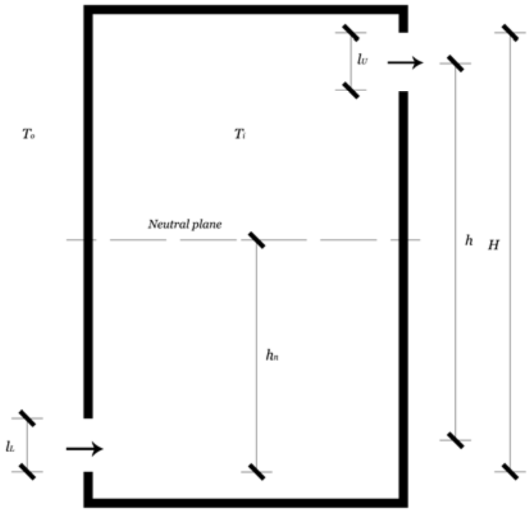

Figure 1 Schematic illustration of the simple physical model considered in this study ($T_i > T_o$)

However, this displacement flow regime is highly dependent of the height of neutral plane, which is defined as the vertical distance at which the internal and external pressures are equal. It has been noticed that, the neutral height is determined by the opening area ratio, $R = A_U / A_L$, where A is the opening area and subscripts U and L designate upper and lower openings respectively. Thus, when the opening area ratio becomes very large/small, the neutral level may increase/decrease dramatically and intersect with upper/lower opening. Under this circumstance, mixing flow regime will be resulted and the pressure distribution along the height of openings cannot be assumed as uniform (See Figure 2). Haslavsky et al. (2006) carried out a series of experiments in a full-scale enclosure for the study of the interactive phenomenon between displacement ventilation and mixing ventilation. It was found that the interaction did exist and a quantitative model for the determination of the interaction was also proposed.

The purpose of the present paper is to further investigate the impacts of the openings of a room on the performance of buoyancy-driven ventilation, with particular focus on how they influence the flow mode, bulk airflow rate and neutral level.

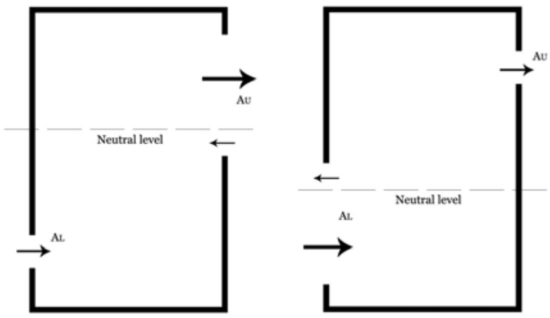

Figure 2 Schematic illustration of the interaction between displacement ventilation and mixing ventilation (left: neutral plane intersects with the upper opening; right: neutral plane intersects with lower opening)

THEORETICAL ANALYSIS

A room with small openings only

The model illustrated in Figure 1 is used for the analysis here. For simplicity, the internal air temperature is considered as uniformly distributed. For an opening like air vent and opening windows, the air flow tends to be approximately turbulent under normal pressures (Awbi 2003). In this case, the airflow rate through an opening approximates to a simple square root law as expressed in Equation (1) (Etheridge and Sandberg 1996):

$$q = C_D A \sqrt{2\Delta p / \rho} \tag{1}$$

where q is the airflow rate, C_D is the discharge coefficient, A is the opening area, Δp is the pressure difference and ρ is the air density. As the heights of both openings are negligible, the overall pressure difference is caused by the density difference between the inside and outside air and can be calculated by Equation (2):

$$\Delta p = \Delta \rho g h = (\rho_o - \rho_i) g h \tag{2}$$

where subscripts o and i designate the outside and inside air respectively, g is the gravity acceleration and h is the vertical distance between the higher and lower openings.

Based on the loop equation method (Axley 1998), the airflow rate can be calculated as follows:

$$q = (C_D A)^* \sqrt{2(\rho_o - \rho_i) g h / \rho_o} \tag{3}$$

where $$(C_D A)^* = \left[\frac{1}{(C_{DU} A_U)^2} + \frac{1}{(C_{DL} A_L)^2} \right]^{-\frac{1}{2}} \tag{4}$$

Assuming that the air temperature is inversely proportional to the pressure based on ideal gas law, the pressure term can then be cancelled and the equation becomes:

$$q = (C_D A)^* \sqrt{2(T_i - T_o) g h / T_i} \tag{5}$$

The height of neutral plane can be determined by:

$$h_n = \frac{\gamma^2}{1+\gamma^2} h \tag{6}$$

where h_n is the height of neutral plane and γ is the opening ratio and is calculated by:

$$\gamma = C_{DU} A_U / C_{DL} A_L \tag{7}$$

It can be seen from this equation that the neutral height is only determined by the vertical distance between the openings and the opening area ratio, and it is not related to the pressure or air temperature. Equation (4) for the calculation of the effective area $(C_D A)^*$ also suggests that the flow rate is more significantly influenced by the smaller opening as it determines the magnitude of the effective area (Linden 1999). However, if the area of lower opening increases, γ will decrease and h_n will decrease as well according to Equation (6). Thus it is possible for the neutral level to intersect with the lower opening if the area of the lower opening continues to enlarge to certain extent. If this happens, the equations introduced above for the calculation of airflow rate and neutral height will be violated as the flow regime has changed.

A room with large openings

It could be seen from the above analysis that the position of the neutral level generally controls the flow regime in the building. Consequently, three flow modes can be defined in terms of the position of the neutral plane:

(I) when the neutral height is at intermediate level of the lower opening;

(II) when the neutral height has no intersection with openings;

(III) when the neutral height is at the intermediate level of the higher opening.

The pressure distributions inside and outside the building for these three modes can be illustrated in Figure 3. As the pressure distributions for large openings cannot be assumed as constant, a multiple element approach has to be adopted, i.e. an opening is divided into small parallel sub-openings and flow rates are calculated individually for each sub-opening, thus the overall airflow rate can be considered as the integration of that of all the small elements. Detailed description of the basic theory for the analysis of large openings is introduced by Li et al. (2000).

Define that H is overall vertical distance from the lower edge of the lower opening to the upper edge of the higher opening and D is the depth of the room. Only 2-D situation is considered.

For flow mode (I), the pressure difference at the higher opening can be obtained by:

$$\Delta p = \int_{H-h_n-l_U}^{H-h_n} \Delta\rho g dh \quad (8)$$

where l is the height of the opening. Thus by substituing Equation (8) into (1) and by integration, the airflow rate through upper opening can be calculated as:

$$q_U = \frac{2}{3}(C_D D\sqrt{2\Delta\rho g/\rho_o})\left[(H-h_n)^{\frac{3}{2}} - (H-h_n-l_U)^{\frac{3}{2}}\right] \quad (9)$$

Considering the energy balance equation for the building and boussinesq approximation, we have:

$$E = \rho C_p q \Delta T \quad (13)$$

$$\Delta\rho/\rho_o = \Delta T/T_o \quad (14)$$

By substituting Equations (13) and (14) into (12), it can be obtained that:

$$q = (\frac{2}{3}C_D D)^{\frac{2}{3}}(\frac{2gE}{T_o C_p \rho})^{\frac{1}{3}} h_n \quad (15)$$

By the same token, we can obtain the following equation for the prediction of the neutral level of flow mode (II):

$$h_n^{\frac{3}{2}} - (h_n - l_L)^{\frac{3}{2}} = (H-h_n)^{\frac{3}{2}} - (H-h_n-l_U)^{\frac{3}{2}} \quad (16)$$

and the equation for airflow rate calculation:

$$q = (\frac{2}{3}C_D D)^{\frac{2}{3}}(\frac{2gE}{T_o C_p \rho})^{\frac{1}{3}}\left[h_n^{\frac{3}{2}} - (h_n - l_L)^{\frac{3}{2}}\right]^{\frac{2}{3}} \quad (17)$$

For flow mode (III), we have:

$$h_n^{\frac{3}{2}} - (h_n - l_L)^{\frac{3}{2}} = (H-h_n)^{\frac{3}{2}} - (h_n + l_U - H)^{\frac{3}{2}} \quad (18)$$

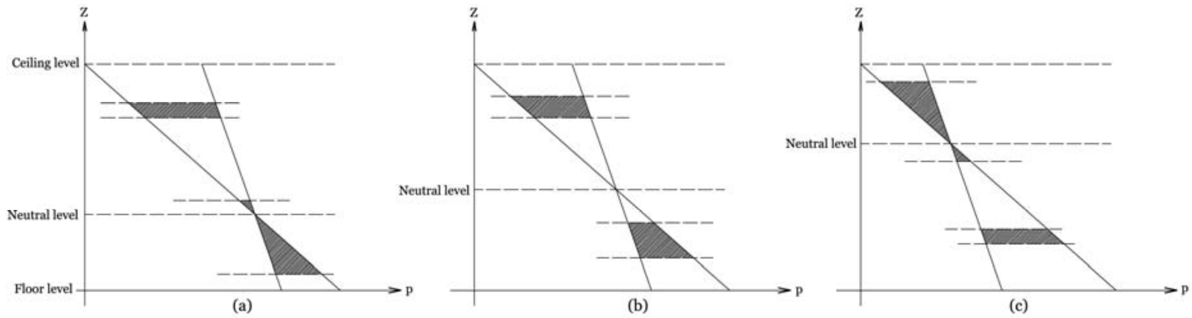

Figure 3 Pressure distributions inside and outside a room with large openings (a: flow mode I; b: flow mode II; c: flow mode III)

Likewise, the airflow rate through the lower opening can be expressed as:

$$q_L = \frac{2}{3}(C_D D\sqrt{2\Delta\rho g/\rho_o})\left[h_n^{\frac{3}{2}} - (l_L - h_n)^{\frac{3}{2}}\right] \quad (10)$$

Thus, by equating the airflow rates through higher and lower openings, we have:

$$h_n^{\frac{3}{2}} - (l_L - h_n)^{\frac{3}{2}} = (H-h_n)^{\frac{3}{2}} - (H-h_n-l_U)^{\frac{3}{2}} \quad (11)$$

The airflow rate of the building can be expressed by the airflow rate below the neutral level, i.e. the incoming flow rate:

$$q = \frac{2}{3}(C_D D\sqrt{2\Delta\rho g/\rho_o})h_n^{\frac{3}{2}} \quad (12)$$

$$q = (\frac{2}{3}C_D D)^{\frac{2}{3}}(\frac{2gE}{T_o C_p \rho})^{\frac{1}{3}}(H-h_n) \quad (19)$$

It can be seen from Equations (11), (16) and (18) that, similar to the situation of small openings, when large openings are incorporated, the neutral level is still determined by the distance between the higher and lower openings and the opening sizes, and it is not related to the temperature difference between the inside and outside air. Nevertheless, the neutral height cannot be calculated with only opening area ratio and overall height. The absolute height of each opening is also important, as the flow mode cannot be decided with the opening ratio and the overall vertical distance only.

In order to calculate the airflow rate, it is necessary to make clear the neutral level first so that the flow mode can be determined and the appropriate equation can be chosen. However, because of power 3/2, it is not possible to obtain analytical solution for Equations (11), (16) and (18) directly. Fortunately, it can be noticed that, for all of them, the left hand side is a monotonically increasing function while the right hand side is a monotonically decreasing one. This suggests that only one solution exist for each of them and numerical approach can be employed for each set of H, l_L and l_U .

Consider a model illustrated as Figure 1 and start with the situation when both openings are of equal size. Thus initially the neutral height is exactly at the middle level between the two openings. When we increase the height of the lower opening l_L , according to Equation (16), the value of the left hand side function will increase, and thus the neutral level will reduce in order to increase the value of function of the right hand side to keep the equation. The further increase of the lower opening area will further result in the reduction of the neutral height and at some point the neutral plane will meet with the upper edge of the lower opening. At this stage, $h_n = l_L$ and equations (16) and (11) become the same.

If we continue to increase the lower opening area, the equation (11) applies and by the similar analysis of above, it could be inferred that the neutral height will increase because the sign of l_L in Equation (11) is opposite to that of Equation (16). This means that, if the height of the higher opening l_U and the overall vertical distance H are fixed, there is a lowest position for neutral plane and this occurs when the neutral plane is of the same height with the upper edge of the lower opening. For the same reason, when the lower opening size and the overall vertical distance are fixed, there would be a highest level of neutral plane if we increase the area of the upper opening.

More interestingly, if we substitute l_U with l_L and l_L with l_U for all equations regarding to the neutral height, it can be easily find that the new solution for these equations have the following relationship with original solution:

$$h_n = H - h_{n,original} \tag{20}$$

This means that, by exchanging the location of the two openings, the flow mode will not be changed. Comparison between equation (15) and (19) suggests that the airflow rate will not be altered as well by doing so. The whole airflow is just ‘rotated’ an angle of 180º.

It can also be seen that, with the increase of lower opening area, the air flow rate will increase as well, no matter which mode the airflow is. Nevertheless, different flow modes have different increasing rate, as Equation (15), (17) and (19) differ from each other. Equations (15) and (19) show that, when bi-directional flows occur, the airflow rate will be linearly proportional to the height of the neutral level. It is also worth mentioning that, when large openings are incorporated, the airflow rate may not be influenced very significantly by smaller openings, as bi-directional flow can occur and some part of the larger opening can complement the area shortage of the small opening.

CFD SIMULATION

Cases investigated

The basic geometry used in CFD simulations has a similar configuration of the one illustrated in Figure 1. It is 12m wide and 12m high. Only 2-D simulation is carried out. Two groups of simulations are performed. In the first group, the size of the higher opening is fixed as 1m and the area of the lower changes from 1m to 7m. In the other group the size of lower opening is fixed as 1m and the area of the higher opening changes from1m to 7m.

In order to study the impacts of opening characteristics and the interaction between different flow modes, the conditions for the openings cannot be assumed as known in the first place. Thus, the computational domain of the CFD simulation has to be extended to include some outside environment. This study found that the minimum dimension for the domain should be 60m wide and 24m high, as shown in Figure 4.

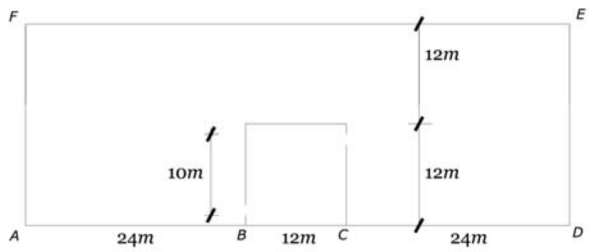

Figure 4 Details of the computational domain and the geometry used for the CFD simulation

The governing equations

The equations solved by CFD are basic mathematical statements of three fundamental physical principles, which are respectively conservation of mass, Newton’s Second Law and conservation of energy. They can be written as follows:

$$\frac{\partial \rho}{\partial t} + \frac{\partial}{\partial x}(\rho \overline{u}) + \frac{\partial}{\partial x}(\rho \overline{v}) + \frac{\partial}{\partial x}(\rho \overline{w}) = 0 \tag{21}$$

$$\frac{\partial}{\partial t}(\rho \overline{u}) + \frac{\partial}{\partial x}(\rho \overline{u}\overline{u}) + \frac{\partial}{\partial y}(\rho \overline{v}\overline{u}) + \frac{\partial}{\partial z}(\rho \overline{w}\overline{u}) = -\frac{\partial \overline{P}}{\partial x} + \frac{\partial}{\partial x_j}\left[(\mu + \mu_t)\left(\frac{\partial \overline{u}}{\partial x_j} + \frac{\partial \overline{u}_j}{\partial x}\right)\right] \tag{22}$$

$$\frac{\partial}{\partial t}(\rho\bar{v})+\frac{\partial}{\partial x}(\rho\overline{uv})+\frac{\partial}{\partial y}(\rho\overline{vv})+\frac{\partial}{\partial z}(\rho\overline{wv})= -\frac{\partial\bar{P}}{\partial y}+\frac{\partial}{\partial x_j}\left[(\mu+\mu_t)\left(\frac{\partial\bar{v}}{\partial x_j}+\frac{\partial\bar{u}_j}{\partial y}\right)\right] \quad (23)$$

$$\frac{\partial}{\partial t}(\rho\bar{w})+\frac{\partial}{\partial x}(\rho\overline{uw})+\frac{\partial}{\partial y}(\rho\overline{vw})+\frac{\partial}{\partial z}(\rho\overline{ww})= -\frac{\partial\bar{P}}{\partial z}+\frac{\partial}{\partial x_j}\left[(\mu+\mu_t)\left(\frac{\partial\bar{w}}{\partial x_j}+\frac{\partial\bar{u}_j}{\partial z}\right)\right]-\rho g\beta(\bar{T}_\infty-\bar{T}) \quad (24)$$

$$\frac{\partial}{\partial t}(\rho c_p\bar{T})+\frac{\partial}{\partial x}(\rho c_p u\bar{T})+\frac{\partial}{\partial y}(\rho c_p v\bar{T})+\frac{\partial}{\partial z}(\rho c_p w\bar{T})= \frac{\partial}{\partial x_j}\left[\left(k+\frac{c_p\mu_t}{\sigma_t}\right)\frac{\partial\bar{T}}{\partial x_j}\right]+q''' \quad (25)$$

The Boussinesq model is used to approximate the relationship between the density and temperature change. The turbulent viscosity μ_t is determined using a two-equation k-ε turbulence model. Following many widely recognised precedents (e.g. Cook 1998; Cook et al 2005), RNG k-ε turbulence model of Yakhot et al. (1992) is employed. The governing equations are discretised with finite volume method.

To increase the stability of the solution process and aid convergence, an unsteady-state approach is used to obtain a steady-state solution and the time scale for each step is calculated according to (Bejan 1995):

$$\Delta t \approx \frac{\tau}{4}=\frac{L}{4\sqrt{g\beta\Delta TL}} \quad (26)$$

where Δt is the time step, L is the characteristic length of the simulation model which is the building height for this study, β is thermal expansion coefficient of air and ΔT is the temperature difference of the inside and outside air.

A robust and commercially available CFD program, FLUENT is used to implement the above methods. Segregated solver is used and PRESTO! is selected as method for the pressure discretisation, as recommended by (FLUENT 1996). Second order approximations are used for the solution of algebraic equations. The default settings of convergence criteria, i.e., the residuals of 10^{-3} for all variables, are adopted.

Boundary conditions

The "fictitious" walls, AF and DE shown in Figure 4 are specified as solid plates with slip boundary conditions and a temperature equal to the outdoor air temperature. The upper boundary, EF, is specified as zero pressure boundary at the outside air temperature. The outside ground, AB and CD are specified as adiabatic. The outside temperature is specified as 17 ℃ (290K) and the interior floor is specified as the heat source and it is 15℃ warmer than the outside. With this heated floor, the air can be considered as mixed: there is no significant vertical temperature stratification (Gladstone and Woods 2001), which complies with the conditions for the theoretical analysis earlier. All the other building walls are regarded as adiabatic.

Validation

A simple validation is performed by comparing the simulation results with the calculations of the theoretical analysis introduced earlier. Consider the case where both openings are 1m high. The convective heat transfer coefficient is specified as 4.0, according to (Denton and Wood 1979). This value also generally complies with the experimental algorithms from other references such as (CIBSE 1988) and (Khalifa and Marshall 1990). The discharge coefficient is assumed to be 0.61. With all these data, it can be calculated using equation (14) that the bulk airflow rate should be 0.40m/s. This value is very close to the airflow rate reported by CFD, 0.37m/s. The discrepancy between simulation and theoretical calculation is less than 10%. This good agreement increases the credibility of both CFD inplementation with settings introduced above and the theoretical analysis before.

RESULTS AND ANALYSIS

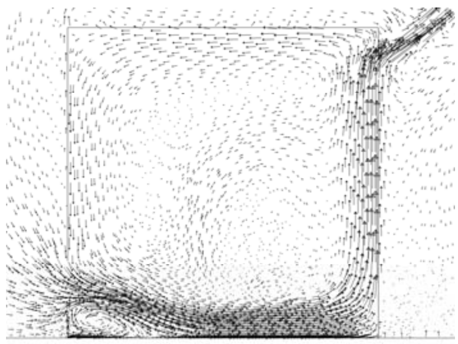

Figure 5 Air flow field when the lower opening height is 2m and the high opening is 1m

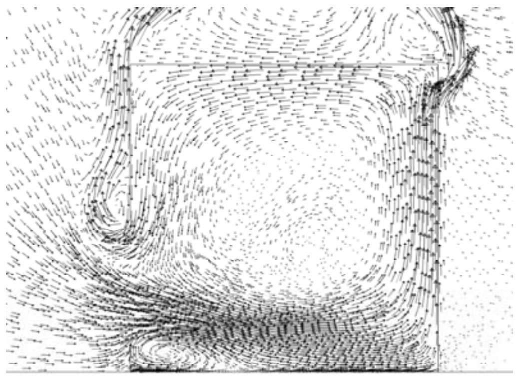

Figure 6 Air flow field when the lower opening height is 5m and the high opening is 1m

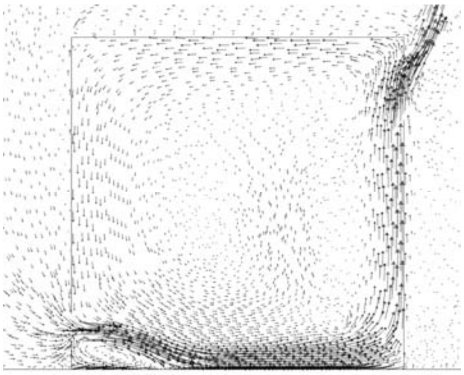

Figure 7 Air flow field when the lower opening height is 1m and the high opening is 2m

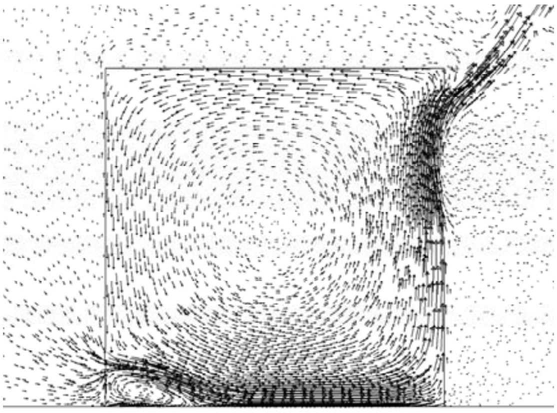

Figure 8 Air flow field when the lower opening height is 1m and the high opening is 5m

Above figures show the air flow fields with different openings sizes. When the opening area ratio is big/small enough, bi-directional flow occurs for larger openings (See Figures 6 and 8), although the flow patterns inside the buildings for them are quite different. When the opening area ratio is at intermediate level then the airflow will be the displacement ventilation (See Figures 5 and 7). These results confirm the theoretical analysis on the general flow regime performed earlier.

Figure 9 shows quantitatively the height of neutral plane and the airflow rate predicted by both theoretical calculation with formulae developed earlier and CFD simulation when the height of the upper opening is 1m and the size of the lower opening changes. Good agreement between the two methods has been achieved with only minor discrepancies for the prediction of the neutral plane when lower opening area is small. The flow mode for these situations is displacement ventilation, i.e. flow mode (II). The discrepancy is partly attributed to the fact there is no simple and direct approach to determine the neutral height for CFD simulation. In this study, this is done by comparing the vertical static pressure distribution of the central line in the building and that of far field. However, as the flow has significant impacts on the pressure distributions, the result is very sensitive to the selection of the lines for comparison. This problem does not exist for bi-directional flow modes (I) and (III), because for these circumstances the neutral level can be easily determined by the position on the opening where the x-velocity is zero. But still, general trend of the change of the height of neutral plane with the increase of the lower opening size is clearly shown.

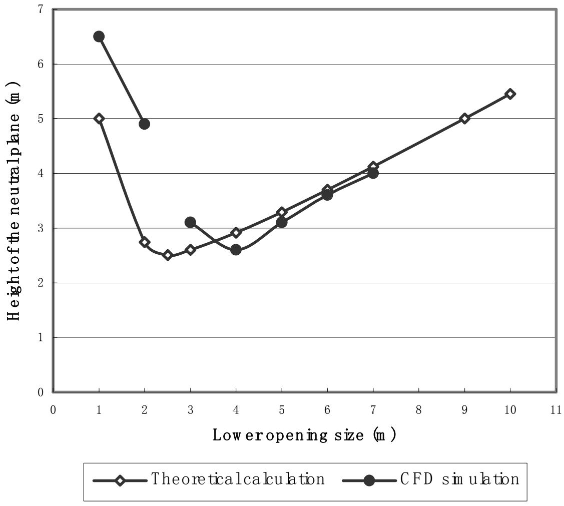

(a)The neutral level predicted by theoretical analysis and CFD simulation

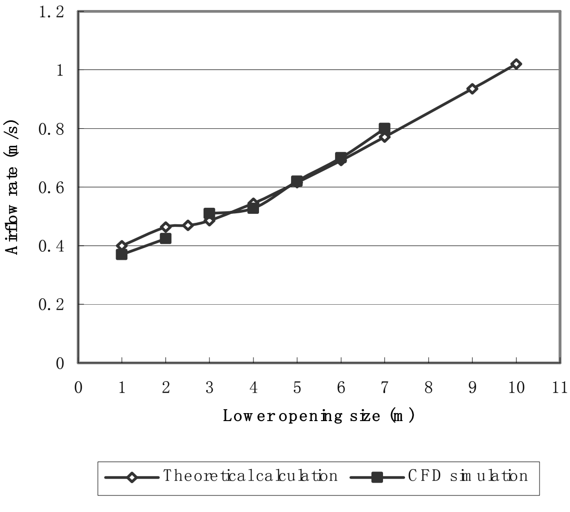

(b)The airflow rate predicted by theoretical analysis and CFD simulation

Figure 9 Comparison of the neutral level and airflow rate obtained from theoretical calculation and CFD simulation (the height of the upper opening is constantly 1m)

It can also be seen from the above figure that, with the increase of the lower opening area from 1m, the neutral level reduces dramatically and when the opening area increases to about 2.5m, the neutral level reaches to the lowest level and the flow mode switches from (II) to (I). Then the height of the neutral plane increases almost linearly with the increase of the area of the lower opening. The airflow rate continuously increases with the increase of the lower opening area and the increasing rate keeps nearly constant all the time, even when the opening area ratio is very small (1/10). This confirms the results of former theoretical analysis and suggests that increasing the area of larger openings may be still an efficient way to enhance the airflow rate because the flow mode has changed and the part of the larger opening can assist the small opening.

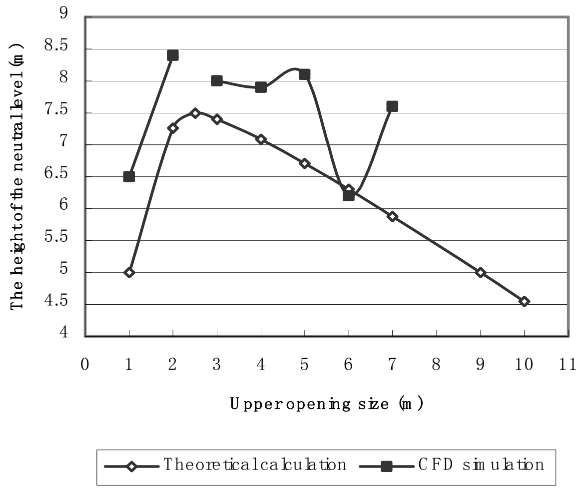

(a)The neutral level predicted by theoretical analysis and CFD simulation

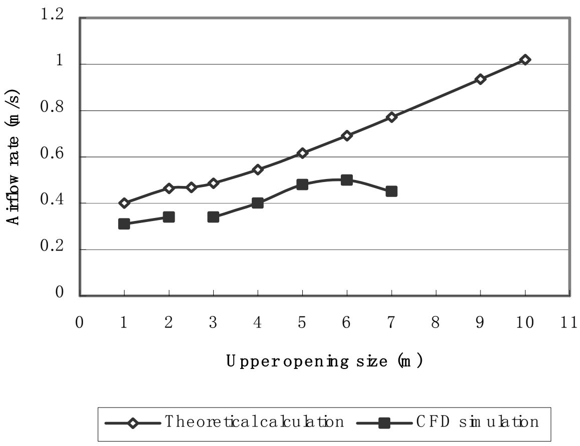

(b)The airflow rate predicted by theoretical analysis and CFD simulation

Figure 10 Comparison of the neutral level and airflow rate obtained from theoretical calculation and CFD simulation (the height of the lower opening is constantly 1m)

The height of the neutral level and the airflow rate predicted by theoretical calculation and CFD simulation are compared in Figure 10 for the case when the height of the lower opening is fixed and that of the higher opening is varied. Generally speaking, agreement on the quantitative trend of the change of the neutral height and the airflow rate is shown but significant discrepancy does exist, especially for the predication of the neutral height. The reason for this might be that, the air movement at the upper opening is much more complicated than that at the lower opening: the vertical momentum around this area is much stronger than the horizontal momentum because of the buoyancy force, which means that, the convective momentum becomes very significant and hence the basic mechanism that the earlier theoretical analysis is based on, the static pressure difference, may not be the only dominant force any longer, especially when the area of upper openings is very large (See Figure 10.a, when the upper opening height exceeds 4m).

The strong vertical momentum at the upper opening also impede the oncoming air to get in the building, thus the theoretical calculation generally over-predicts the airflow rate, compared to CFD simulation. At certain point, increasing the upper opening area has little effect on the airflow rate (See Figure 10.b, when the upper opening height exceeds 5m).

CONCLUSIONS

This paper investigates the buoyancy-driven natural ventilation of a room with large lower and higher level openings. Conventional models for buildings with small openings usually employ the assumption that the heights of the openings are negligible and thus only displacement ventilation can happen in the space. However, this assumption is not appropriate when large openings are incorporated, especially when bi-directional flow for an opening occurs.

According to the relationship between the neutral height and the openings, three flow modes can be identified: (I) when the neutral height is at intermediate level of the lower opening; (II) when the neutral height has no intersection with openings; (III) when the neutral height is at the intermediate level of the higher opening. Regarding each of the above flow mode, pressure-based formulae have been developed to predict the height of neutral plane and the airflow rate.

These formulae suggest that the height of the neutral plane is determined by the overall vertical distance between the openings, the absolute size of each opening other than the openings area ratio used for small openings model. For a fixed upper/lower opening area, there is a lowest/highest level for the neutral plane. Airflow rate increases with the increase of the openings and large openings also have a significant impact on the airflow rate, as they can change the flow mode and hence assist the small opening.

CFD simulation was performed in order to verify the theoretical analysis and good agreement was achieved both qualitatively and quantitatively for flow mode (I), i.e. when the neutral level intersects with the lower opening. However, there are significant discrepancies between the CFD simulation and theoretical prediction for flow mode (III), although to some extent they show the same trend for the change of airflow rate and neutral height when the upper opening increases/decreases. This may be caused by the strong vertical momentum transfer at the upper opening due to the buoyancy force, which changes the dominant force from static pressure difference to convective forces.

It was also shown in the CFD simulation that, in order to increase the airflow rate, increasing the area of the lower opening is more efficient than increasing that of the upper opening. Nevertheless, it should be noted that doing so will significantly reduce the neutral height, which may be expected to be very high for some purposes: for instance, atrium spaces are often used as buffer zones to help the ventilation of the adjacent buildings and thus the neutral height should be very high so that the air in adjacent buildings can be sucked into the atrium and then expelled from upper openings. As a result a compromise may have to be made to keep the balance.

REFERENCES

Anderson, K. T. (2003). "Theory for natural ventilation by thermal buoyancy in one zone with uniform temperature." Building and Environment 38.

Awbi, H. B. (2003). Ventilation of buildings. London, New York, Spon Press, Taylor & Francis Group.

Axley, A. (1998). Introduction to the design of natural ventilation systems using loop equations. Proceedings of 19th AIVC conference, Oslo, Norway.

Bejan, A. (1995). Convection heat transfer. New York ; Chichester, J. Wiley.

Chen, Z. D. and Y. Li (2002). "Buoyancy-driven displacement natural ventilation in a single-zone building with three-level opening." Building and Environment(37).

CIBSE (1988). CIBSE Guide. Chartered institute of Building Services Engineering, UK.

Cook, M. J. (1998). An evaluation of computational fluid dynamics for modelling buoyancy-driven displacement ventilation. Leicester, De Montfort University.

Cook, M. J., Y. Ji, et al. (2005). CFD modelling of buoyancy-driven natural ventilation opposed by wind. Proceedings of 9th IBPSA Conference, Montreal, Canada.

Denton, R. A. and I. R. Wood (1979). "Turbulent convection between two horizontal plates." International Journal of Heat and Mass Transfer 22.

Etheridge, D. and M. Sandberg (1996). Building ventilation : theory and measurement. Chichester ; New York, John Wiley & Sons.

Fitzgerald, S. D. and A. W. Woods (2004). "Natural ventilation of a room with vents at multiple levles." Building and Environment 39.

FLUENT (1996). Fluent: user's guide. Lebanon, N.H., Fluent Incorporated.

Gladstone, C. and A. W. Woods (2001). "On buoyancy-driven natural ventilation of a room with a heated floor." Jounal of Fluid Mechanics 441.

Haslavsky, V., J. Tanny, et al. (2006). "Interaction between the mixing and displacement modes in a naturally ventilated enclosure." Building and Environment 41.

Khalifa, A. J. N. and R. H. Marshall (1990). "Validation of heat transfer coefficients on interior building surfaces using a real-sized indoor test cell." International Journal of Heat and Mass Transfer 33(10).

Li, Y. (2000). "Buoyancy-driven natural ventilation in a thermally stratified one-zone building." Building and Environment(35).

Li, Y., A. Delsante, et al. (2000). "Prediction of natural ventilation in buildings with large openings." Building and Environment 35.

Linden, P. F. (1999). "The fluid mechanics of natural ventilation." Annual Reviews of Fluid mechanics 31.

Linden, P. F., G. F. Lane-Serff, et al. (1990). "Emptying filling boxes: the fluid mechanics of natural ventilation." Jounal of Fluid Mechanics 212.

Yakhot, V., S. A. Orszag, et al. (1992). "Development of turbulence models for shear flows by a double expansion technique." Phys. Fluids 4.